INL/CON-13-29297
PREPRINT

# Insights into Cold Water Injection Stimulation Effects Through Analytical Solutions to Flow and Heat Transport

## 37th GRC Annual Meeting

Mitchell Plummer

September 2013

The INL is a
U.S. Department of Energy
National Laboratory
operated by
Battelle Energy Alliance

# Insights into Cold Water Injection Stimulation Effects through Analytical Solutions to Flow and Heat Transport

**Mitchell Plummer, Idaho National Laboratory**

**Keywords: cold water injection, thermal stimulation, injectivity, permeability enhancement**

## Introduction

Wells in traditional hydrothermal reservoirs are used to extract heat and to dispose of cooled water. In the first case, high productivity (the ratio of production flow rate to the pressure differential required to produce that rate) to is preferred in order to maximize power generation, while minimizing the parasitic energy loss of pumping. In the second case, high injectivity (the change in injection flow rate produced from a change in fluid injection pressure) is preferred in order to reduce pumping costs. In order to improve productivity or injectivity, cold water is sometimes injected into the reservoir in an attempt to cool and contract the surrounding rock matrix and thereby induce dilation and/or extension of existing fractures or to generate new fractures. Though the increases in permeability associated with these changes are likely localized, by improving connectivity to more extensive high-permeability fractures they can, at least temporarily, provide substantially improved productivity or injectivity.

The effects of cold water injection on injectivity have been observed at many sites, and the data demonstrate that changes in injectivity can be relatively large. Gunnarsson (2011), for example measured increases in injectivity in the Hellisheidi field, SW Iceland of more than six times when the water injection temperature was lowered from 120°C to 20°C even while viscosity at the injection temperature would have been ~5 times greater. Grant et al. (2013), in a review of field data, from thermal stimulation tests, demonstrated a nonlinear relationship between injectivity and water injection temperature and noted that field data commonly demonstrate an injectivity increase that is proportional to $t^n$, where t is time and n is between 0.4 and 0.7.

## Analysis of Cold Water Injection Effects

While a number of recent studies have modeled a variety of processes that are likely occur under a cold water injection stimulation effort (eg. Nygren and Ghassemi 2006, Ghassemi et al. 2008, Podgorney et al. 2011) , the conclusions of such studies provide results that are quite specific to the simulation scenario constructed and provide only limited insight into the general nature of the effects of cold water injection. Elsworth (1989) provided a more general treatment of the effects of cold water injection on blocky rock masses using an analytical solution for heat flow in the matrix combined with finite element solution of the fluid and heat flow equations. That work, however, focused on permeability enhancement and did not discuss some of the implications for injectivity that are of interest here. The goal of this paper is to elucidate why changes in

injectivity may occur during cold water injection and how the fracture distribution affects those changes. We therefore take a similar approach to that of Grant et al (2013) who provided a relatively simple mathematical analysis of how injectivity would be expected to change during cold water injection stimulation by considering propagation of a cooling front and consequent contraction of rock in a permeable porous medium. In our analysis, however, we use commonly applied analytical solutions for heat transport tin in fractured rock to illustrate how and why injectivity increases while viscosity also increases.

We consider two relatively simple fracture networks, in hopes that the results may be generalized to more realistic systems. To simplify later discussion, and provide results with obvious relationship to real systems, we define some common characteristics for each of two hypothetical fracture systems considered. Specifically, we consider a fractured hydro-stratigraphic unit 200 m in thickness, with a horizontal permeability of 2E-2 millidarcy [2E-17 $m^2$], yielding a transmissivity of 4 m millidarcy, [4E-12 $m^3$]. For the stimulation, we consider a 30-day injection of 60°C water into a reservoir initially at 140°C, with a flow rate into the formation of 13.25 L $s^{-1}$. Other parameters used in the calculations, but which are generally less variable between systems, are given in Appendix A.

To illustrate how the number of fractures conducting water flow in the reservoir governs the response of the system to cold water injection, we consider – for each geometric model – fracture sets comprised of 1, 10 and 100 fractures. The aperture of each fracture is then calculated from the cubic law for transmissivity of a fracture (Domenico and Schwartz, 1990) with aperture, b:

$$b = \left( \frac{12Tr}{N_f} \right)^{1/3}, \qquad \text{Eq. 1}$$

where Tr is the total transmissivity provided by the number of fractures, $N_f$, providing flow, where each fracture is actually an interconnected set of fractures providing an independent flow path.

The first system considered is a collection of infinite, parallel, horizontal, planar fractures with a vertical extent confined to an arbitrary vertical extent representative of a fractured geologic unit. A schematic of the system, for a single fracture in the hypothetical layered system is shown as Figure 1. Initially, we assume that the fractures are uniformly spaced and that the spacing between the fractures is

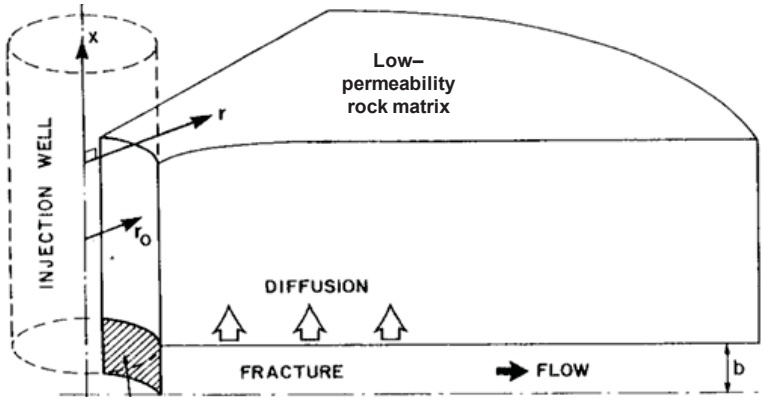


**Figure 1. Schematic illustrating the geometry of the radial flow into a set of parallel, uniformly spaced, horizontal infinite fractures, from Feenstra et al. (1984).**

greater than the penetration of the cooling front into the rock between the fractures during the cold water injection period. Under these conditions, the cooling of the rock and fracture can be calculated using an analytical solution of the advection dispersion equation for radial flow (Feenstra et al. 1984). For the single-fracture radial flow scenario, Figure 2 illustrates the relative temperature distribution in the rock at the conclusion of the injection period, where relative temperature is defined as

$$T_{rel} = \frac{T - T_{inj}}{T_{res} - T_{inj}}, \qquad \text{Eq. 2}$$

and T is temperature, $T_{inj}$ is the injection temperature and $T_{res}$ the background reservoir temperature. For cases of 1, 10 and 100 fractures, Figure 3A shows the relative temperature along a single fracture path, illustrating that for constant injection rate, the extent of penetration of the cooling front decreases dramatically with the number of fractures providing flow away from the injection point.

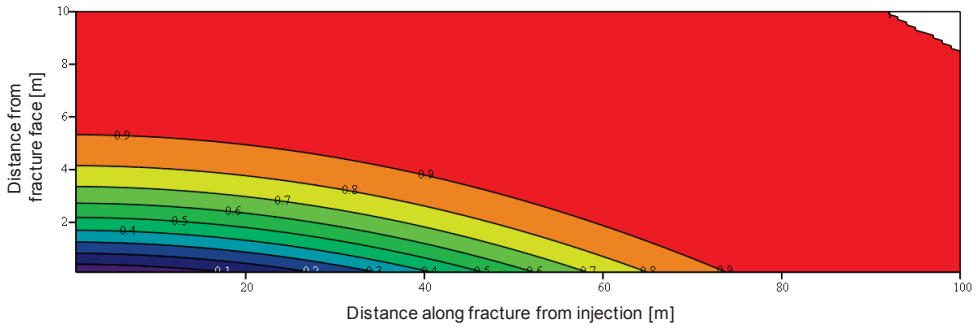


**Figure 2. Distribution of relative temperature in the rock adjacent to a fracture in the radial flow scenario. Injection well is located at the origin.**

As Figure 2 demonstrates, the vertical extent of cooling is greatest immediately adjacent to the well. The thermal penetration at that location can be estimated from the characteristic thermal diffusion length (eg. Kirby 2010), L:

$$L = \sqrt{D_{th} t_{inj}}, \qquad \text{Eq. 3}$$

where $D_{th}$ is the thermal diffusivity of the matrix and $t_{inj}$ is the duration of the cold water injection. This characteristic length gives the distance to which the half the temperature difference will propagate during the injection period. As the number of fractures in the hypothetical fractured hydrostratigraphic unit increases, the interfracture spacing decreases, and when the distance between fractures approaches this characteristic length, thermal interference between cooling fronts parallel to the fracture face becomes important.

Because we assume a constant flow rate the overall velocity also decreases as the number of fractures conducting flow increases and the distance that the cooling front propagates decreases with increasing fracture number (Figure 3A). However, because the velocity is also inversely proportional to fracture aperture, and aperture is nonlinearly related to the number of fractures via the cubic law, the water flux through the fractures is essentially proportional to $N^{-2/3}$. Thus a ten-fold increase in the number of fractures diminishes the propagation of the cooling front by a factor of about 5.

To examine the maximum effect that cooling is likely to have on fracture dilation, we assume that the stress regime around the rock allows the matrix to freely contract and dilate as cooling progresses. Grant et al. (2013) and Elsworth (1989) employed similar assumptions in their analyses of permeability enhancement associated with thermal strain in fractured rock. The change in aperture, Δb, is then calculated by integrating the thermal strain across the interfracture spacing,

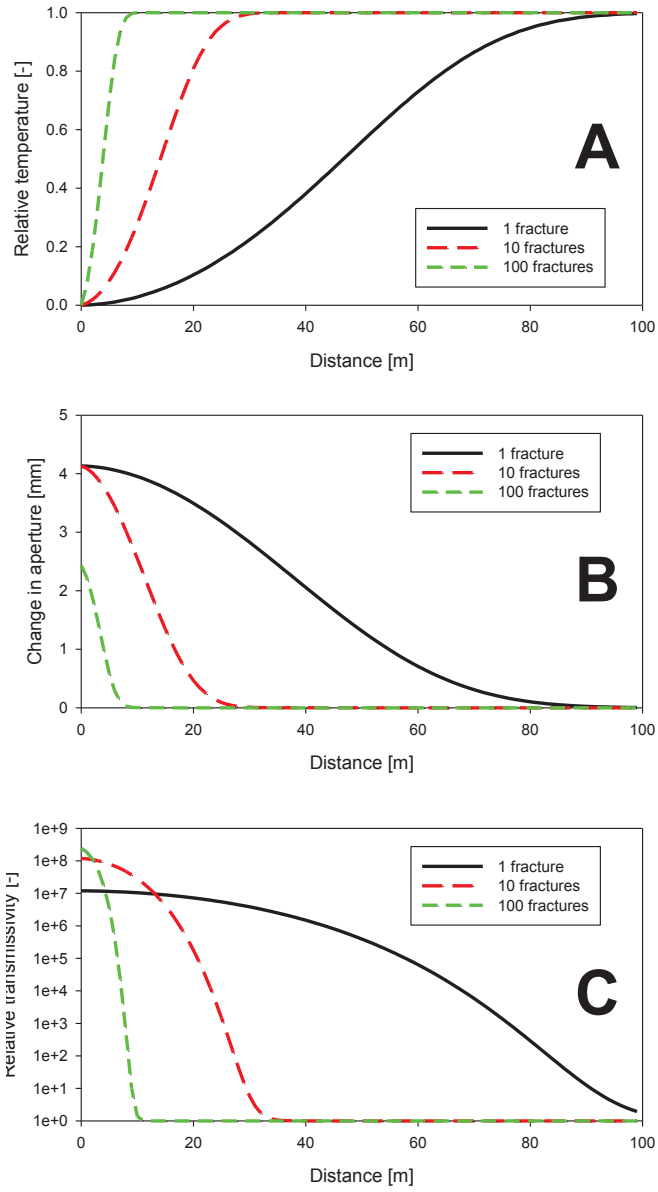


**Figure 3. Plots illustrating response of a radial flow fracture system to a 30-day cold water injection period, for (A) relative temperature, (B) aperture change and (C) relative transmissivity.**

$$\Delta b = \int_0^B (\beta \cdot T_{rel} \cdot \Delta T) dz \qquad \text{Eq. 4}$$

where B is the interfracture spacing, β is the coefficient of thermal expansion, $\Delta T_{inj}$ is the difference between injection and ambient reservoir temperature, $T_{rel}$ is the relative temperature, and z is the distance into the rock normal to the fracture face. The resulting changes in fracture aperture (Figure 3b) are very large relative to its intial value (Table 1); in each fracture set considered, the initial aperture is less than 0.1 mm but the aperture dilation in the cooled region is on the order of several mm. We calculate the effect on the local transmissivity using the cubic law, which demonstrates that transmissivity can increase by many orders of magnitude in the

region where the rock adjacent to the fracture is cooled to a significant distance into the rock (Figure 3c).

**Table 1. Fracture and flowparameters for a hypothetical injection into a system of parallel horizontal fractures (radial flow) and into a system of parallel vertical fractures (1D flow).**

| N | Aperture [mm] | Fracture spacing [m] | Fracture density [1/m] | Velocity at injection face [m/s] | | Increase in injectivity [-] at $t_{inj}$ | | Thermal penetration distance [m] at $t_{inj}$ | |
|---|---|---|---|---|---|---|---|---|---|
| | | | | Radial | 1D | Radial | 1D | Radial | 1D |
| 1 | 0.036 | 200 | 0.005 | 58 | 1.8 | 320 | 2.8E5 | 93 | 180 |
| 10 | 0.017 | 20 | 0.05 | 13 | 0.39 | 4.2 | 1.3 | 30 | 18 |
| 100 | 0.0078 | 2 | 0.5 | 2.7 | 0.09 | 2.1 | 1.0 | 2 | 1 |

Contraction of the rock is likely to take place much faster than the process of cooling, so it is reasonable to assume a quasi-static permeability response to cooling. The cooling front also propagates much more slowly than the advection front itself, so changes in storage associated with the injection are, at any time, occurring at much greater distances from the well than the distance to which the cooling front has propagated. We can thus calculate the effect on fluid pressure in the cooled region of the fracture assuming that the pressure gradient accommodates all of the flow. The pressure gradient required to accommodate the flow is then a function only of the flow rate, fluid viscosity and fracture transmissivity. While we include the viscosity dependence on temperature in these calculations, the viscosity increases only by a factor of two between the initial reservoir temperature (140°C) and injection temperature (60°C).

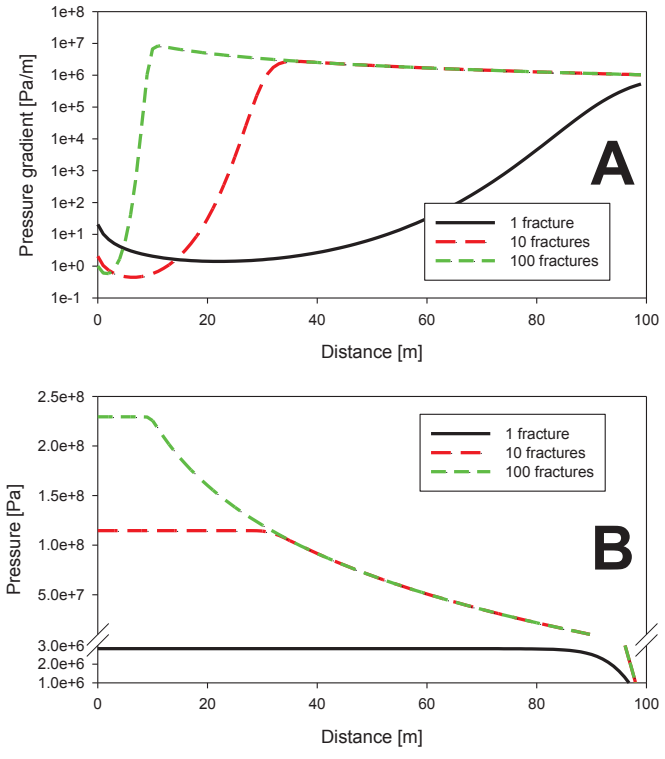


**Figure 4. Plots illustrating response of a radial flow fracture system to a 30-day cold water injection period, for (A) pressure gradient and (B) pressure.**

The large changes in transmissivity produced by the dilation of the surrounding rock easily dominate the increasing viscosity associated with cooling, and dramatically decrease the gradient required to accommodate the specified flow rate (Figure 4A). The effect

on fluid pressure at the well (Figure 4B), however, is much less pronounced than the effect on permeability and pressure gradient, because that pressure at any point along the flow path represents the integral of the pressure gradient across the distance from the distal reference point to the well. The region of dramatically increased transmissivity effectively reproduces the effect of a very large well bore, with a flat spot in the pressure vs. distance curve that extends through the region of cooled rock. The change in the well head pressure is thus largely controlled by the shape of the initial pressure vs. distance curve, and the distance to which the cooling front has propagated. For the radial flow problem, the pressure gradient declines logarithmically with distance from the well, so the maximum injectivity increase results from cooling proximal to the well. However, because the velocity of the cooling front increases inversely proportional to, and nonlinearly with, the number of fractures (again, because we specify constant flow rate), the injectivity increases dramatically as the number of fractures decreases. Thus, for the radial flow problem, the injectivity at the end of the injection period has increased by a factor of more than 300 for the single fracture case, but only by a factor of 4 and 2, respectively, for the 10-fracture and 100-fracture cases (Table 1).

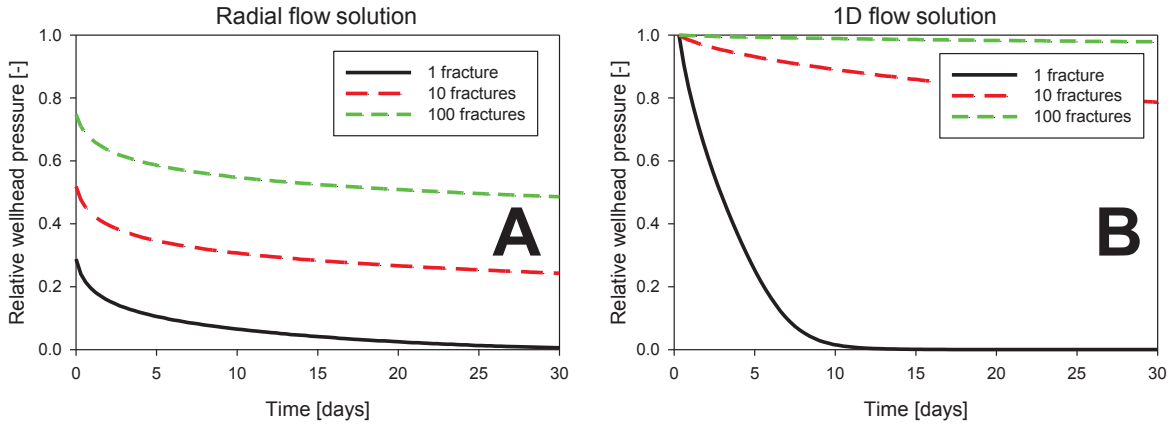


**Figure 5. Plots illustrating relative wellhead pressure vs time for the radial and 1-D flow systems, during the 30-day cold water injection period.**

The change in injectivity as a function of time (Figure 5A) is also largely controlled by the shape of the initial pressure vs distance curve, so that injectivity increases fastest at early time, as the transmissivity in the smallest radial cross section is increased. Thus, for the constant flow rate considered here , injection pressure declines quickly in early time and the rate of decline slows dramatically after less than approximately half a day, as the cooling front propagates quickly through the near-wellbore region. The observed decrease in pressure at the well with time is approximately proportion al to $t^{0.3}$, slightly lower than the range of exponents for that relationship as found in Grant et al.'s recent (2013) review of field data.

The second system considered is a set of parallel, vertical, planar fractures of effectively infinite length but with vertical extent the same as the first system. Figure 7 illustrates a conceptual model for such a system, in which the injection well is connected (via horizontal drilling or a

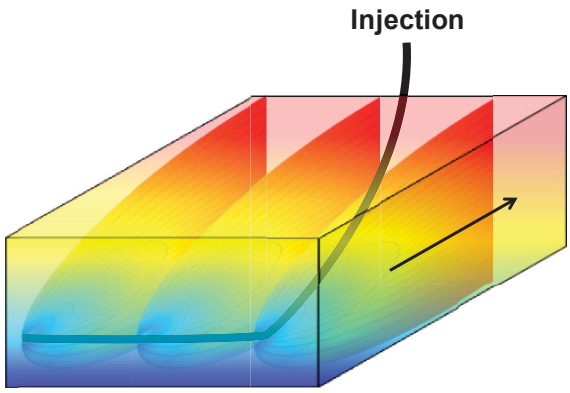


**Figure 7. Schematic illustrating the conceptual model for flow in a set of vertical, parallel, uniformly spaced fractures for the 1D horizontal flow model. Color illustrates rock temperature during cooling via cold water injection.**

separate fracture) to the ends of a series of parallel fractures. Flow in such a system, where the length is much greater than the fracture height, is largely one dimensional, and the velocity is thus again related to the number of assumed fractures, their aperture and the fracture height. The velocity in this case is, however, essentially constant along the flow paths, so the cooling behavior is quite distinct from that of the radial flow model. For the case of parallel, uniformly space fractures, we calculate the propagation of the cooling front with the Gringarten solution (Gringarten and Witherspoon 1975). For the cases considered, however, we assume that the extent of the fracture rock perpendicular to flow is the same as the vertical dimension (200 m), so the fracture spacing, as in the radial flow case (Table 1), except for the 100-fracture case, is larger than the characteristic thermal diffusion length. As a result, the temperature vs distance curves (Figure 6) are essentially identical to those computed using the Carslaw and Jaeger (1959) solution, for 1D flow in fractures in which cooling is independent of that in other fractures.

The relationship between propagation distance of the cooling front and number of fractures is quite different for the 1D flow case than the radial flow case, because the velocity does not decrease with radial distance in the latter scenario. The propagation distance of the cooling front is thus directly proportional to the number of fractures into which the flow is divided, so that the cooling front for the single fracture case extends 100 times as far as for the 100-fracture case (Table 2, Figure 6A. The sensitivity of the injectivity of the system to the number of fractures conducting flow is also larger than for the radial flow case. At the prescribed transmissivity, the cooling front penetrates only a couple of meters for the 100-fracture case, but extends to almost 200 m for the single fracture case.

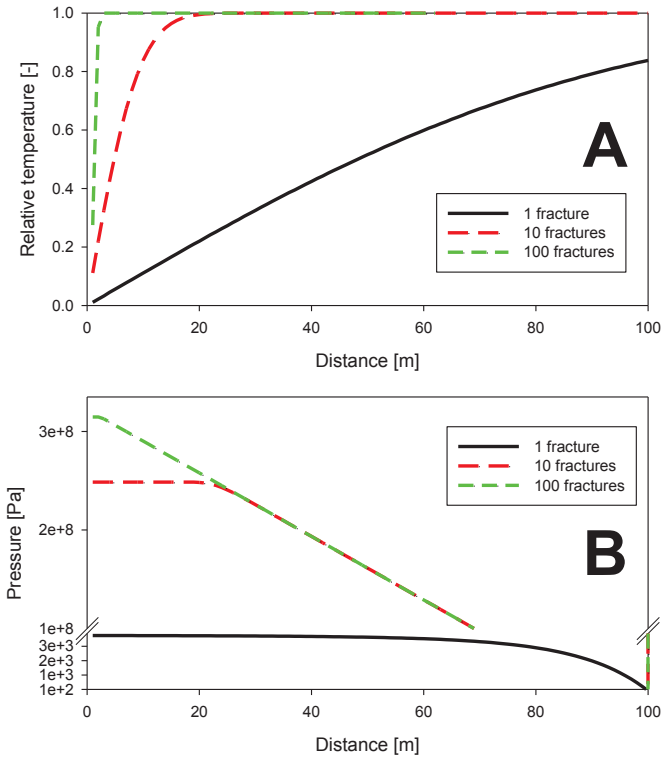


**Figure 6. Plots illustrating response of a 1D flow system in parallel fractures to a 30-day cold water injection period, for (A) relative temperature and (B) pressure.**

Unlike the radial flow case, the pressure decline with distance for this fracture network geometry is linear, so the primary control on increasing injectivity is through propagation of cooling. This yields a distinctly different pressure vs time curve (Figure 5B) for the 1D flow case than for the radial flow case, with a nearly constant rate of pressure decline until some boundary is reached that minimizes any further propagation. In real reservoirs, even where fractures distribution may at some point yield dominantly unidirectional flow, a radial flow pressure distribution will exist in the region that distributes flow to that network of fractures. This latter example is thus most useful as an illustration of how the pressure distribution dictated by the fracture network can affect injectivity as the thermal front migrates through that network.

## Conclusions

The simple analysis presented here provides a simple explanation for the increase in injectivity associated with cold water injection and demonstrates that even neglecting the effects of fracture generation, fracture dilation associated with thermal strain can profoundly alter the permeability of a fractured system in the region. Moreover, we illustrate that particularly for constant flow tests, changes in injectivity are heavily influenced by the initial pressure distribution around the injection well, as well as the extent to which the cooling front alters permeability.

For realistic flow and heat transport parameters, in a case where the number of interconnected fractures that conduct flow away from a well is on the order of 10 to 100, we illustrate that a 30-day cold water injection could cause increases in injectivity of a factor of 2 to 4, with larger increases associated with fewer fractures. Changes of similar magnitude were observed in the cold water injection tests at the Hellisheidi field, SW-Iceland (Gunarsson 2011). These estimates of fracture number, or of large-scale fracture density and fractured zone extent, are useful because they give some insight into the number of interconnected independent fracture paths extending from a well, and these estimates can in some cases be tested via interwell tracer tests, which constrain flowpath velocities. We conclude that the method of analysis presented here provides useful insight into the effects of cold water injection on injectivity and suggest that is also a simple and effective means of estimating how measured changes in injectivity may be related to fracture number and/or density.

## References

Carslaw, H.S., and J.C. Jaeger (1959), *Conduction of Heat in Solids*. Oxford University Press, Oxford, U.K., 510 p.

Domenico, P.A. and F.W. Schwartz (1990) Physical and Chemical Hydrogeology, John Wiley and Sons, Section 3.4, p. 87.

Elsworth, D. (1989) Thermal permeability enhancement of blocky rocks: One-dimensional flows, Int. J. Rock Mech. Min Sci. & Geomech. Abstr., Vol. 26, No. 3/4, pp. 329-339.

Feenstra, S., J. Cherry, E. Sudicky and Zia Haq (1984) Matrix diffusion effects on contaminant migration from an injection well in fractured sandstone, Groundwater, Vol. 22, No. 3, pp. 307-316.

Ghassemi, A., A. Nygren and A. Cheng. (2008) Effects of heat extraction on fracture aperture: A poro-thermoelastic analysis, Geothermics, Vol. 37, No. 5, pp. 525-539.

Grant, M.A., (2012) "Thermal stimulation: the easiest and least recognised mechanism of permeability change" Paper presented at US/NZ geothermal workshop

Grant, M.A., J. Clearwater, J. Quinao, P.F. Bixley, and M.L. Brun (2013) Thermal stimulation of geothermal wells: A review of field data Proc., 38th Workshop on geothermal reservoir engineering, Stanford University

Gringarten, A.C., P.A. Witherspoon, and Y. Ohnishi (1975), "Theory of heat extraction from fractured hot dry rock." Journal of Geophysical Research. Vol. 80, No.8, pp. 1120-1124.

Gunnarson, G., (2011) "Mastering reinjection in the Hellisheidi field, SW-Iceland: a story of successes and failures" Proc., 36th Workshop on geothermal reservoir engineering, Stanford University

Kirby, B. (2010) *Micro- and Nanoscale Fluid Mechanics – Transport in Microfluidic Devices*, New York: Cornell University.

Nygren, A., Ghassemi, A., & Cheng, A., (2005) Effects of cold-water injection on fracture aperture and injection pressure, Transactions, Vol. 29, Geothermal Resources Council

Nygren, A. and A. Ghassemi (2006) Poroelastic and Thermoelastic Effects of Injection into a Geothermal Reservoir, 41st U.S. Symposium on Rock Mechanics (USRMS), June 17 - 21, 2006 , Golden, CO.

Podgorney, R., Gunnarson, G., & Huang, Hai, 2011 "Numerical simulation of temperature dependent fluid reinjection behaviour, Hellisheidi geothermal field, Southwest Iceland." Transactions, v35, Geothermal Resources Council